Mice carrying a human *GLUD2* gene recapitulate aspects of human transcriptome and metabolome development

Qian Li[a,b,1], Song Guo[a,1], Xi Jiang[a], Jaroslaw Bryk[c,2], Ronald Naumann[d], Wolfgang Enard[c,3], Masaru Tomita[e], Masahiro Sugimoto[e], Philipp Khaitovich[a,c,f,4], and Svante Pääbo[c,4]

[a]Chinese Academy of Sciences Key Laboratory of Computational Biology, Chinese Academy of Sciences-Max Planck Partner Institute for Computational Biology, Shanghai Institutes for Biological Sciences, Chinese Academy of Sciences, 200031 Shanghai, China; [b]University of Chinese Academy of Sciences, 100049 Beijing, China; [c]Max Planck Institute for Evolutionary Anthropology, 04103 Leipzig, Germany; [d]Max Planck Institute of Molecular Cell Biology and Genetics, D-01307 Dresden, Germany; [e]Institute for Advanced Biosciences, Keio University, 997-0035 Tsuruoka, Yamagata, Japan; and [f]Skolkovo Institute for Science and Technology, 143025 Skolkovo, Russia

Edited by Joshua M. Akey, University of Washington, Seattle, WA, and accepted by the Editorial Board April 1, 2016 (received for review September 28, 2015)

Whereas all mammals have one glutamate dehydrogenase gene (*GLUD1*), humans and apes carry an additional gene (*GLUD2*), which encodes an enzyme with distinct biochemical properties. We inserted a bacterial artificial chromosome containing the human *GLUD2* gene into mice and analyzed the resulting changes in the transcriptome and metabolome during postnatal brain development. Effects were most pronounced early postnatally, and predominantly genes involved in neuronal development were affected. Remarkably, the effects in the transgenic mice partially parallel the transcriptome and metabolome differences seen between humans and macaques analyzed. Notably, the introduction of *GLUD2* did not affect glutamate levels in mice, consistent with observations in the primates. Instead, the metabolic effects of *GLUD2* center on the tricarboxylic acid cycle, suggesting that *GLUD2* affects carbon flux during early brain development, possibly supporting lipid biosynthesis.

human evolution | *GLUD2* | brain metabolism

Glutamate dehydrogenase (GDH) is a metabolic enzyme catalyzing the conversion of glutamate to α-ketoglutarate and ammonia (1). Whereas the ammonia is metabolized via the urea cycle, the α-ketoglutarate enters the tricarboxylic acid (TCA) cycle in mitochondria. Besides its metabolic role, glutamate also functions as a major excitatory neurotransmitter (2, 3).

Whereas most organisms contain one copy of the *GLUD* gene encoding the GDH enzyme, humans and apes have two: *GLUD1* and an additional gene, *GLUD2*, which originated by retroposition of the *GLUD1* transcript after the split from apes and old world monkeys (4). Sequence analysis suggests that it is highly unlikely that *GLUD2* would have contained an intact ORF and a K_a/K_s <1 throughout the evolution of apes without being functional (5). Moreover, positive selection has affected *GLUD2* (4), including changes in amino acid residues that make it less sensitive to low pH and GTP inhibition, and resulting in a requirement for high ADP levels for allosteric activation (4, 6, 7). *GLUD2* mRNA expression levels in tissues are lower than those of *GLUD1*, but similarly distributed across tissues. However, whereas the ancestral version of the *GLUD* enzyme occurs both in mitochondria and the cytoplasm, *GLUD2* is specifically targeted to mitochondria (8, 9).

Changes in *GLUD2* properties have been suggested to reflect functional adaptation to the metabolism of the neurotransmitter glutamate in the brain (4, 10), and the fact that *GLUD2* has been positively selected and maintained during ape and human evolution suggests that it may have physiological effects important for the function of ape and human brains. However, the connection between the emergence of the *GLUD2* gene in the ancestors of apes and humans and changes in brain function remains elusive. To date, the only direct insights into *GLUD2* function come from a rare *GLUD2* mutation linked to the onset of Parkinson's disease (11) and from glioma cells carrying a mutated isocitrate dehydrogenase 1 gene (*IDH1*) where *GLUD2* expression reverses the effects of the *IDH1* mutation by reactivation of the metabolic flux from glucose and glutamine to lipids by way of the TCA cycle (12).

To investigate the physiological role the *GLUD2* gene may play in human and ape brains, we generated mice transgenic for a genomic region containing human *GLUD2*. We compared effects on gene expression and metabolism during postnatal development of the frontal cortex of the brain in these mice and their wild-type littermates, with similar data obtained from humans and rhesus macaques, the closest relative of humans and apes, which lack the *GLUD2* gene.

Results

A Mouse Model of *GLUD2*. We constructed transgenic mice carrying a 176-kb-long human genomic region containing the *GLUD2* gene, as well as 43 kb of upstream and 131 kb of downstream DNA sequences (*SI Appendix*, Fig. S1). To account for effects potentially caused by stochastic insertion of *GLUD2* sequence into the mouse

Significance

A novel version of the glutamate dehydrogenase gene, *GLUD2*, evolved in the common ancestors of humans and apes. Based on sequence and expression pattern, *GLUD2* has been suggested to play a role in glutamate metabolism in human and ape brains. We have generated transgenic mice carrying a human *GLUD2* gene. Analysis of transcriptome and metabolome changes induced by *GLUD2* in the cerebral cortex revealed no changes in glutamate concentration but instead changes to metabolic pathways centering on the TCA cycle during early postnatal development. These changes mirrored differences seen between human and macaque during cortex development, suggesting that *GLUD2* may play a role during brain development in apes and humans, possibly by providing precursors for the biosynthesis of lipids.

Author contributions: W.E., P.K., and S.P. designed research; X.J., J.B., R.N., and M.S. performed research; W.E., M.T., and M.S. contributed reagents/analytic tools; Q.L. and S.G. analyzed data; and Q.L., P.K., and S.P. wrote the paper.

The authors declare no conflict of interest.

This article is a PNAS Direct Submission. J.M.A. is a guest editor invited by the Editorial Board.

Freely available online through the PNAS open access option.

Data deposition: The data reported in this paper have been deposited in the Gene Expression Omnibus (GEO) database, www.ncbi.nlm.nih.gov/geo (accession no. GSE80122).

[1]Q.L. and S.G. contributed equally to this work.

[2]Present address: School of Applied Sciences, University of Huddersfield, HD1 3DH Huddersfield, UK.

[3]Present address: Department of Biology II, Ludwig Maximilians University, 82152 Martinsried, Germany.

[4]To whom correspondence may be addressed. Email: khaitovich@eva.mpg.de or paabo@eva.mpg.de.

This article contains supporting information online at www.pnas.org/lookup/suppl/doi:10.1073/pnas.1519261113/-/DCSupplemental.

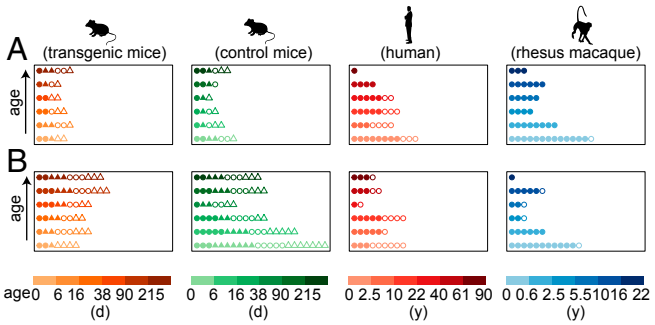

Fig. 1. Sample information. (*A*) Schematic representation of age, sex, and transgenic line information for mouse and primate samples used for transcriptome (RNA-seq) measurements. (*B*) Schematic representation of age, sex, and transgenic line information for mouse and primate samples used for metabolome (CE-MS) measurements. Each symbol represents an individual sample. The colors indicate genotype/species information: orange, transgenic mice; green, control mice; red, humans; blue, rhesus macaques. Lighter shades of color indicate younger ages. The bars show the corresponding age intervals: d, days; y, years. The symbols indicate mice lines: circles, line a; triangles, line b. Filled symbols indicate males; empty symbols indicate females.

genome, we constructed two independent transgenic lines (a and b). Anatomical, neurophysiological, and behavioral analyses of adult mice did not reveal any overt effects of the *GLUD2* genotype in the two lines (13).

We assessed the effects of *GLUD2* on gene expression and metabolite concentrations in the developing frontal cortex of hemizygous ($GLUD2^+$) mice from both lines as well as control littermates, using RNA sequencing (RNA-seq) and capillary electrophoresis coupled with mass spectrometry (CE-MS). RNA-seq data were collected from 30 $GLUD2^+$ and 29 control individuals. Metabolite concentrations were measured in 56 $GLUD2^+$ and 81 control individuals. The mice varied in age from 3 d to 18 mo, with ages and sexes matched between transgenic and control groups (Fig. 1 *A* and *B* and *SI Appendix*, Table S1).

To assess whether molecular changes induced by *GLUD2* in the mice might recapitulate differences between hominoids (apes and humans) and other primates, we measured metabolite concentrations in prefrontal cortex of 35 humans and 31 rhesus macaques using CE-MS. For both species, samples covered the respective lifespans approximately corresponding to the one sampled in the mice: from 16 d postnatal to 90 y in humans, and from 18.4 wk postconception to 21 y in macaques (Fig. 1*B* and *SI Appendix*, Table S2). We furthermore analyzed RNA-seq data previously collected in the prefrontal cortex of 38 humans and 40 rhesus macaques covering the same age span (14) (Fig. 1*A* and *SI Appendix*, Table S2). Between these two datasets, 13 human and 20 macaque individuals overlapped for both the RNA-seq and CE-MS data (*SI Appendix*, Table S2).

***GLUD2* Affects Gene Expression During Early Postnatal Development.** Based on 613 million, 100 nt-long sequence reads collected from the mouse polyA-plus RNA (*SI Appendix*, Table S3), we detected expression of 18,610 protein-coding and noncoding genes. Global expression variation among the samples showed a clear effect of age when analyzed by principal component analysis (PCA), whereas neither genotype nor sex affected gene expression substantially (Fig. 2*A* and *SI Appendix*, Fig. S2). Consistently, as many as 15,663 of the 18,610 detected genes, including the *GLUD2* transgene, showed significant age-dependent expression changes in the mouse cortex [*F*-test, Benjamini–Hochberg (BH) corrected $P < 0.05$, false discovery rate (FDR) < 0.01].

Both transgenic mouse lines showed the same developmental expression profile of *GLUD2*, which was distinct from the expression profile of *GLUD1* (*SI Appendix*, Fig. S3). Notably, the *GLUD2* expression trajectory in the developing mouse brain strongly resembled the trajectory of *GLUD2* expression during prefrontal cortex development in humans (Pearson correlation, $r = 0.86$, $P < 0.0001$; *SI Appendix*, Fig. S4). We also detected expression of a long noncoding RNA (lncRNA) originating from the opposite strand of the transfected human genomic region upstream of the *GLUD2* transcription start site (*SI Appendix*, Fig. S5). Expression profile of this lncRNA closely resembled the expression profile of *GLUD2* (*SI Appendix*, Fig. S6), suggesting that it is expressed from the same bidirectional promoter as *GLUD2* (*SI Appendix*, Table S4).

An effect of the *GLUD2* genotype, albeit small, was detectable: using analysis of covariance (ANCOVA) with linear, quadratic, and cubic models, we identified 12 protein-coding genes and one lncRNA showing significant expression differences between the two transgenic lines and control littermates (*F*-test, BH corrected $P < 0.05$, permutations $P < 0.05$, FDR < 0.01, *SI Appendix*, Table S5). Strikingly, the effect of the *GLUD2* genotype was observed only during early postnatal development and disappeared at approximately 2 wk of age (Fig. 2*B*). By contrast, other genes expressed in the mouse brain did not show any increased divergence between transgenic and control mice during early development (Fig. 2*C*).

Eleven of the 13 genes differentially expressed between transgenic and control mice fell into the same coexpressed module in an unsupervised hierarchical clustering analysis (Fig. 3*A* and *SI Appendix*, Table S5 and Fig. S7), an observation not expected by chance (permutations, $P < 0.001$) (*SI Appendix*, Fig. S8). The genes affected by *GLUD2* are thus coexpressed during mouse development. The expression of these 11 genes decreased rapidly during early postnatal development in both transgenic and control mice, but in the transgenic mice, the decrease in expression was shifted to earlier stages of development (Fig. 3 *B* and *C* and *SI Appendix*, Fig. S9).

Based on analysis of Gene Ontology (GO) terms (15), the 11 coexpressed genes were significantly enriched in several biological processes, many of them related to neural development and transcriptional regulation (hypergeometric test, FDR corrected $P < 0.05$) (Fig. 3*D* and *SI Appendix*, Table S6), a result robust to the use of different background gene distributions. The genes affected by *GLUD2* may thus to some extent be functionally related.

***GLUD2* Effects in the Mice Mirror Differences Between Primates.** To assess whether the effect of *GLUD2* in the mice recapitulated differences between primate species that lack and that have *GLUD2*, we reanalyzed 579 million, 100-nt-long RNA-seq reads from the prefrontal cortex of rhesus macaques and humans. We detected the expression of 23,115 protein-coding and noncoding

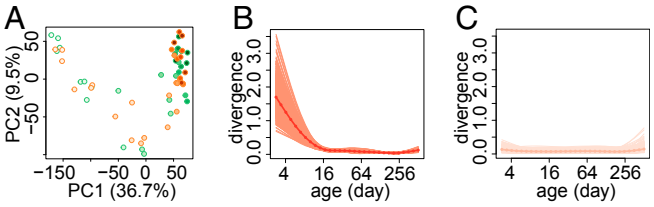

Fig. 2. Effect of the *GLUD2* genotype on gene expression in the mouse model. (*A*) The first two principal components (PCs) of the principal component analysis, based on the expression of 18,610 genes detected in the mouse brain. Each circle represents an individual. The colors indicate genotype information: orange, transgenic mice; green, control mice. Symbols filled by lighter shades of color indicate younger ages. (*B*) The mean normalized gene expression divergence between transgenic and control mice, based on the 13 age-dependent genes with expression affected by the *GLUD2* genotype (red curve). The colored area shows variation of the divergence estimates obtained by bootstrapping the 13 genes 1,000 times. (*C*) The mean normalized gene expression divergence between transgenic and control mice, based on the remaining 15,650 age-dependent genes (light-red curve). The colored area shows variation of the divergence estimates obtained by subsampling 13 genes 1,000 times.

EVOLUTION

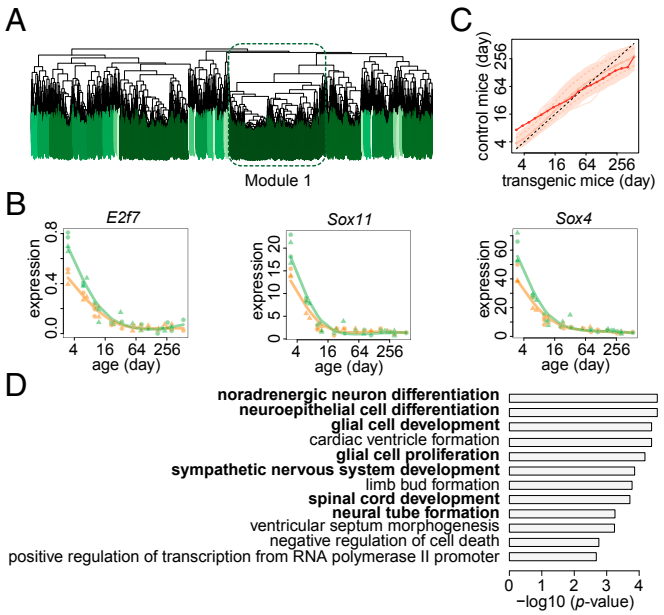

Fig. 3. Patterns and functions of genes with expression affected by *GLUD2* genotype. (*A*) Dendrogram based on unsupervised hierarchical clustering of 15,663 age-dependent genes. The colors represent coexpressed modules. The darker shades of color indicate larger modules. Dashed green rectangle shows module 1 containing 11 of the 13 genes with expression affected by the *GLUD2* genotype. (*B*) Expression profiles of 3 of the 11 module 1 genes with expression affected by the *GLUD2* genotype. Each point represents an individual sample. The colors indicate genotype information: orange, transgenic mice; green, control mice. The symbols indicate mice lines: circles, line a; triangles, line b. The lines show spline curves fitted to expression data points with four degrees of freedom. (*C*) Developmental time shift between transgenic mice and control mice, calculated based on expression of 11 module 1 genes with expression affected by the *GLUD2* genotype (dark-red curve) and the remaining 15,652 age-dependent genes (light-red curve). The light-red–colored area shows variation of time-shift estimates for the remaining age-dependent genes, obtained by randomly subsampling 11 genes 1,000 times. The curves are obtained by aligning transgenic mice expression time series to that of control mice, using the modified dynamic time warping algorithm, showing the ages where transgenic mice expression levels correspond to those of control mice. During early stages of development, transgenic mice ages are mapped to older ages in control mice, indicating transgenic mice expression profiles shift to earlier developmental stages. (*D*) GO biological processes significantly enriched in 11 module-1 genes with expression affected by the *GLUD2* genotype. Biological processes related to neural development are shown in bold.

genes. PCA analysis of the expression of these genes demonstrated substantial species-dependent as well as age-dependent divergence (Fig. 4*A*).

Among the 13 genes differentially expressed between transgenic and control mice, 9 were expressed in human and macaque prefrontal cortex (*SI Appendix*, Table S5). Remarkably, the expression of these 9 genes showed a large divergence between humans and macaques at the earliest stages of postnatal development after which the divergence rapidly decreased. Thus, the expression differences between humans and macaques resembled those seen between mice carrying a *GLUD2* gene and control littermates (Fig. 4*B*). By contrast, other genes expressed in human and macaque prefrontal cortex showed no such divergence pattern (permutation $P = 0.05$, Fig. 4*C*).

Furthermore, seven of the nine genes showed a rapid expression level decrease during human and macaque early postnatal development, i.e., the same developmental expression trajectory as the genes affected by *GLUD2* in the transgenic mice (Pearson correlation, $r > 0.9$, permutation $P < 0.001$, *SI Appendix*, Figs. S10 and S11). After adjusting for the differences in lifespan between humans and macaques, we found a shift in the timing of the expression to earlier developmental stages in humans relative to macaques (Fig. 4*D* and *SI Appendix*, Fig. S10), similar to what is seen in the *GLUD2* mice. This was not caused by any general mismatching of human and macaque developmental timing, as other genes did not show such a coordinated shift to earlier developmental stages (Pearson correlation, $r > 0.9$, permutation $P = 0.02$, *SI Appendix*, Fig. S12). Thus, gene expression changes in *GLUD2* mice indeed recapitulate gene expression differences between human and macaque expression profiles during early postnatal development.

Among the 7 genes showing similar expression and developmental shifts in the transgenic mice and in human cortex, 3 are transcription factors (TFs) implicated in neural development: SRY (sex determining region Y)-box 4 (*SOX4*), SRY (sex determining region Y)-box 11 (*SOX11*), and Distal-less homeobox 2 (*DLX2*) (16–22). A total of 15 known neural-related target genes of these TFs (16–29) were expressed in the mice and 14 in the primates (*SI Appendix*, Table S7). The expression divergence profiles of these target genes and the corresponding TFs between the transgenic and control mice and between humans and macaques at different ages were significantly correlated (Pearson correlation, $r > 0.5$; permutation $P = 0.008$ for mice and $P = 0.001$ for primates, *SI Appendix*, Fig. S13), suggesting that the effects of *GLUD2* may go beyond the 13 genes showing differences between the transgenic and control mice.

As the effects of *GLUD2* in the mice were strongest at the earliest stages of postnatal development, it is possible that *GLUD2* plays a role mainly in prenatal development. To test if this may be the case in humans, we analyzed the expression of the 13 genes affected by *GLUD2* expression in the mice using RNA-seq data from prenatal prefrontal cortex development of humans (30) and macaques. Of the 13 genes, 9 had detectable expression in our human and macaque data, as well as in public fetal human cortex data. Strikingly, expression of the 9 genes was substantially more divergent between humans and macaques before than after birth (Fig. 5 *A* and *B* and *SI Appendix*, Fig. S14), whereas other

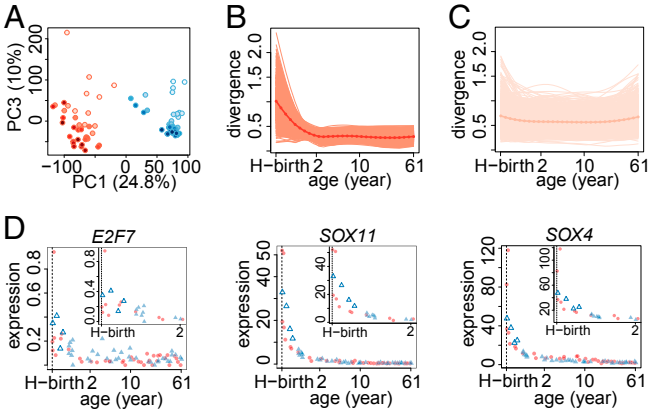

Fig. 4. Gene expression in primates. (*A*) The first and third PCs of the principal component analysis, based on the expression of 23,115 genes detected in human and rhesus macaque prefrontal cortex. Each circle represents an individual (red, humans; blue, macaques). Lighter shades of color indicate younger ages. (*B*) The mean normalized gene expression divergence between humans and macaques based on the 9 genes with expression affected by *GLUD2* genotype in the mouse model (red curve). The colored area shows variation of the divergence estimates obtained by bootstrapping the 9 genes 1,000 times. "H-birth" *x*-axis marks represent human birth age. (*C*) The mean normalized gene expression divergence between humans and macaques based on the remaining 23,106 detected genes (light-red curve). The colored area shows variation of the divergence estimates obtained by subsampling 9 genes 1,000 times. (*D*) Expression profiles of E2F transcription factor 7 (*E2F7*), *SOX11*, and *SOX4*, which are among the 7 genes showing the similar expression and divergence pattern in primates and the transgenic mice. Each point represents an individual. The colors indicate species information: red, humans; blue, macaques. Filled symbols indicate postnatal ages; empty points, prenatal ages. The vertical dashed line shows the human birth age.

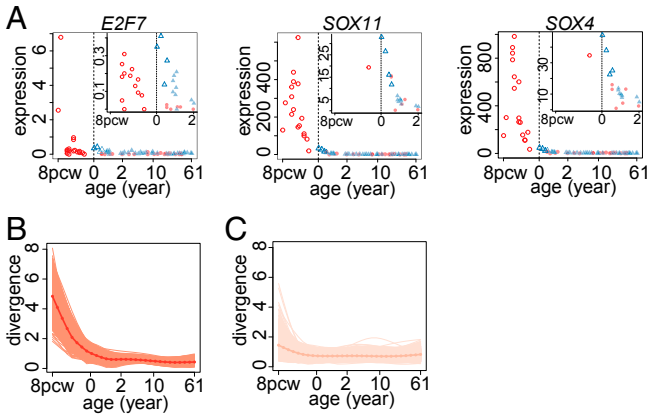

Fig. 5. Prenatal gene expression. (*A*) Prenatal expression profiles of *E2F7*, *SOX11*, and *SOX4* genes, which are among the 7 genes showing similar expression and divergence patterns in primates and the transgenic mice. Each point represents an individual. The colors indicate species information: red, humans; blue, macaques. Filled symbols indicate postnatal ages; empty points, prenatal ages (17 in humans and 4 in macaques). The vertical dashed line shows the human birth age; pcw, weeks postconception. (*B*) The mean normalized gene expression divergence between humans and macaques based on the 9 genes with expression affected by the *GLUD2* genotype, calculated using a published fetal human dataset (red curve). The colored area shows variation of the divergence estimates obtained by bootstrapping the 9 genes 1,000 times. (*C*) The mean normalized gene expression divergence between humans and macaques, based on the remaining 15,897 detected genes in the public fetal human and our macaque time series data (light-red curve). The colored area shows variation of the divergence estimates obtained by subsampling 9 genes 1,000 times.

expressed genes showed no obvious increase in expression differences before birth (Fig. 5*C*).

Brain Metabolism in *GLUD2* Mice and Primates. We assessed the effects of *GLUD2* on metabolism in the brains of the *GLUD2* mice using CE-MS. For comparisons, we similarly analyzed human and macaque brains. We detected and quantified 110 and 88 metabolites in the mice and in humans and macaques, respectively (*SI Appendix*, Tables S8 and S9). PCA analysis based on concentration levels of these metabolites revealed a substantial effect of age in both mice and primates (Fig. 6 *A* and *B*).

We first focused on the concentration levels of glutamate, the direct substrate of the GDH2 enzyme encoded by *GLUD2*. We detected no effect of *GLUD2* on glutamate concentration in the mouse cortex (Fig. 6*C*). By contrast, glutamate concentrations in the prefrontal cortex of the humans are substantially lower than in the macaques (Fig. 6*C*). Previous work using gas chromatography coupled with mass spectrometry (GC-MS) has shown that compared with humans, chimpanzees as well as macaques have higher glutamate levels in the brain (31), something that reexamination of the published glutamate data confirms (Fig. 6*C*). Because both humans and chimpanzees carry *GLUD2* genes, a mechanism other than the mere presence of *GLUD2* must be responsible for the lower glutamate concentrations in the human brain.

Despite the absence of a *GLUD2* effect on glutamate levels in the mice, we detected that the overall differences between the metabolomes of the transgenic and the control mice were about threefold larger shortly after birth relative to 2 mo after birth (*SI Appendix*, Fig. S15). To test if this may be at least partially connected to gene expression differences, we compared the concentration profiles of 24 metabolites associated with the metabolic pathways where the 13 genes differentially expressed between transgenic and control mice are located (*SI Appendix*, Table S8). Concentration differences of the 24 metabolites were substantially larger than the differences for the 86 remaining compounds analyzed (Fig. 7*A*). Similar results were obtained using the Kyoto Encyclopedia of Genes and Genomes (KEGG) pathway annotation and the Small Molecule Pathway Database (32) to identify metabolites and pathways associated with the 13 genes (*SI Appendix*, Fig. S16).

The 13 genes and 24 metabolites showing increased divergence between the transgenic and control mice converged within seven KEGG pathways (*SI Appendix*, Table S10). For three of these pathways, the HIF-1 signaling pathway, the pentose phosphate pathway, and carbon metabolism, metabolite concentration differences were significantly greater than expected by chance (permutations, $P < 0.05$) (Fig. 8*A*). The three pathways are closely related as the "carbon metabolism" pathway includes the pentose phosphate pathway and the TCA cycle, which is in turn linked to the HIF-1 signaling pathway (Fig. 8*B*).

We next analyzed metabolic differences between human and macaque brains. As the human samples were frozen after substantial postmortem delay (PMD), we first analyzed the effects of PMD by comparing three macaque samples that were intentionally collected with substantial PMD with macaque samples that were not (*SI Appendix*, Table S11). Of the 88 metabolites detected in the macaque and human brains, 21 were affected by PMD in at least one of the three samples analyzed (*SI Appendix*, Fig. S17 and Table S9) and were therefore excluded from further analyses.

For the remaining 67 metabolites, the differences between humans and macaques explained 26% of the total variation in metabolite concentrations. By comparison, the *GLUD2* genotype explains 2% of the metabolic variation in the mice (*SI Appendix*, Fig. S18). Despite the much greater overall metabolic differences between macaques and humans than between the transgenic and control mice, it is notable that in both cases, the greatest metabolic differences are seen in early development (*SI Appendix*, Figs. S15 and S19).

Of the 24 metabolites linked to the genes differentially expressed between *GLUD2* and control mice, 11 were among the

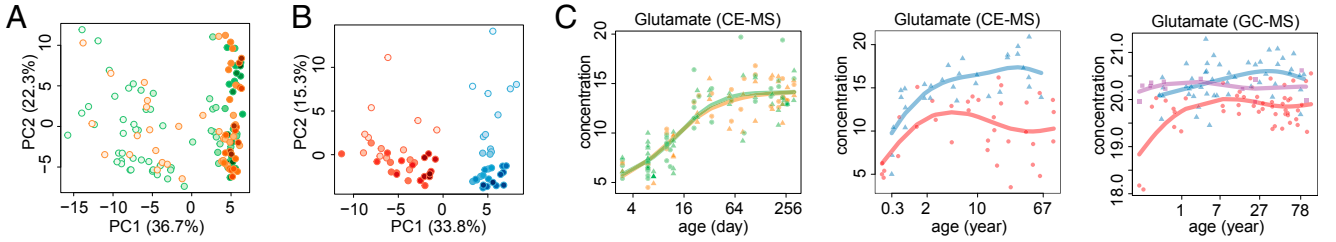

Fig. 6. Metabolite differences and glutamate concentration among genotypes/species. (*A* and *B*) The first two PCs of the principal component analysis, based on the concentrations of 110 metabolites detected in mouse frontal cortex and 88 metabolites detected in human and macaque prefrontal cortex. Each circle represents an individual. The colors indicate genotype/species information: orange, transgenic mice; green, control mice; red, humans; blue, rhesus macaques. Lighter shades of color indicate younger ages. (*C*) Glutamate concentration profiles measured in mice using CE-MS and in primates using CE-MS and GC-MS. The colors indicate genotype/species information as in *A* and *B*; purple, chimpanzees. Lines show spline curves fitted to concentration data points with four degrees of freedom.

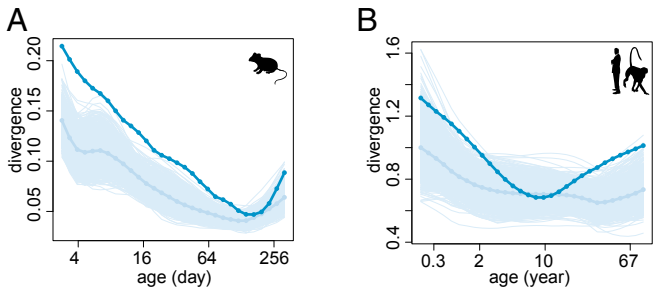

Fig. 7. Metabolome analyses of transgenic mice and primates. (*A*) The mean normalized metabolite concentration divergence between transgenic and control mice, based on the 24 metabolites sharing the same KEGG pathway as the 13 genes with expression affected by the *GLUD2* genotype (dark-blue curve) and the remaining 86 detected metabolites (light-blue curve). The colored area shows variation of the divergence estimates of the 86 metabolites obtained by bootstrapping 1,000 times. (*B*) The mean normalized metabolite concentration divergence between humans and macaques based on 11 of the 24 metabolites linked to the *GLUD2* genotype effect in mice (dark-blue curve) and the remaining 56 detected metabolites (light-blue curve). The colored area shows variation of the divergence estimates of the 56 metabolites obtained by bootstrapping 1,000 times.

67 metabolites that were detected and unaffected by PMD in humans and rhesus macaques (*SI Appendix*, Table S9). As in the mice, these 11 metabolites diverged more between humans and macaques than the other detected metabolites in early development (Fig. 7*B*). However, this effect was less pronounced in development and also apparent at later age, possibly due to fewer metabolites detected in the primates than in the mice, as well as differences in lifespan. Still, for 8 of the 11 metabolites detected in both primates and mice, the direction of concentration change coincided between humans and transgenic mice (permutation, $P = 0.08$) (*SI Appendix*, Fig. S20). Thus, *GLUD2* transgenic mice recapitulate some of the metabolic differences seen between human and macaque brains.

Discussion

GLUD2 originated as an evolutionary novel version of the glutamate dehydrogenase gene as a result of the retroposition of a *GLUD1* transcript in the common ancestors of humans and apes. We investigated the function of *GLUD2* by inserting the human *GLUD2* gene and surrounding sequences carrying putative regulatory elements into the mouse genome. We isolated two independent transgenic lines to exclude artifacts caused by the insertion of the human gene in the mouse genome. When analyzed in the frontal cortex, both lines displayed similar developmental *GLUD2* expression trajectories, closely resembling *GLUD2* expression in human prefrontal cortex during development.

In both transgenic lines, *GLUD2* affects the expression of 13 genes, 11 of which show similar ontogenetic expression profiles. These genes include several TFs, among which *DLX2*, *SOX4*, and *SOX11* play important roles in neuronal differentiation and neurogenesis (16, 18, 19, 25). Some of the previously described targets of these TFs show changes in expression in the transgenic mice that are correlated with expression changes of the corresponding TFs. Nine primate orthologs of the 13 mouse genes affected by *GLUD2*, including *DLX2*, *SOX4*, and *SOX11*, differ in expression between human and macaque ontogenesis in ways that mirror the changes seen in the mice. Similarly, primate orthologs of target genes of *DLX2*, *SOX4*, and *SOX11* show expression differences correlating with those of these TFs. These results illustrate that the introduction of *GLUD2* into the mouse genome induces effects paralleling evolutionary differences between primate species that carry a *GLUD2* gene and those that do not. This adds to a mounting amount of evidence suggesting that human-specific variants of genes such as *FOXP2*, *ASPM*, *EDAR*, *SRGAP2*, and *CMAH* can be fruitfully studied in mouse models (33).

The gene expression changes induced by *GLUD2* in the mice and the differences between humans and macaques were restricted to early development and were not observed past the first 2 wk postpartum in the mice or the first 2 y of life in humans.

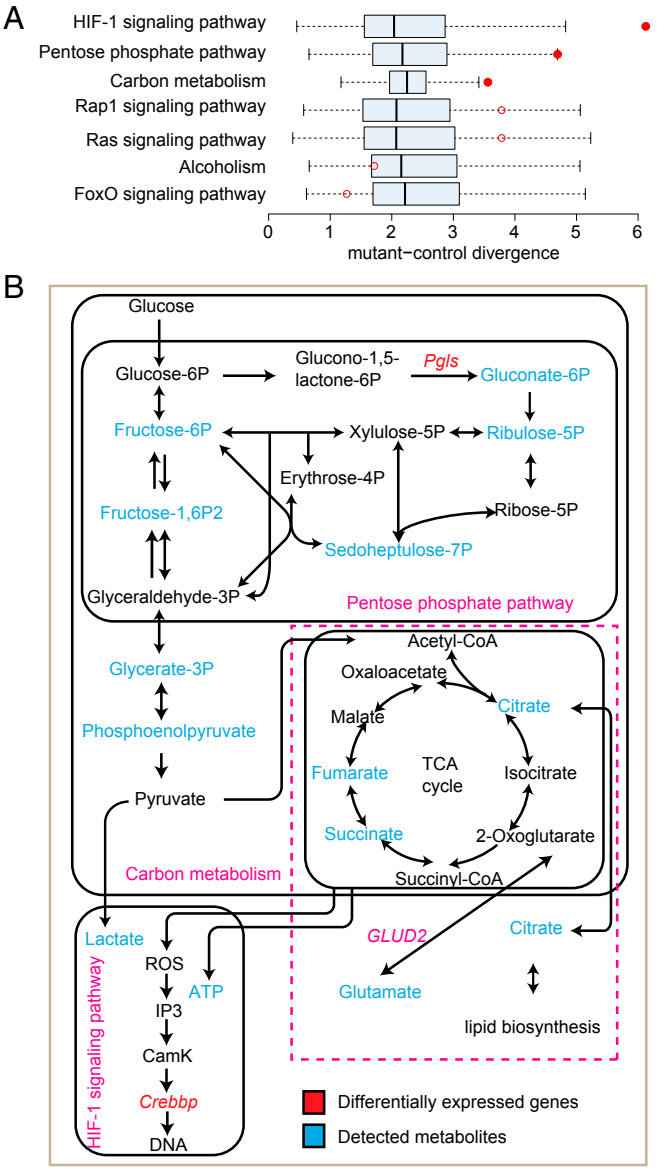

Fig. 8. Pathway analysis of the *GLUD2* genotype effect on mouse metabolome. (*A*) Metabolite concentration divergence between transgenic and control mice, based on metabolites in a pathway (red circles). The boxplots show metabolite concentration divergence between transgenic and control mice, calculated by sampling 1,000 times the same number of metabolites as detected in a given pathway from the bulk of remaining detected metabolites. Each pathway contains at least two detected metabolites and at least one gene differentially expressed between transgenic and control mice. The filled circles show the pathways with significantly greater metabolic divergence than expected by chance. (*B*) The schematic representation of the three KEGG pathways showing significantly greater metabolite concentration divergence between transgenic and control mice: HIF-1 signaling pathway, pentose phosphate pathway, and carbon metabolism. Detected metabolites are shown in blue and genes with expression affected by the *GLUD2* genotype are shown in red. Dashed pink rectangle delineates the pathway affected by *GLUD2* overexpression in *IDH1*-mutant glioma cells.

This suggests that *GLUD2* mainly functions during brain growth and early development, a notion that is in apparent contradiction to the idea that *GLUD2* has a major role in the metabolism of the neurotransmitter glutamate.

The metabolic data lend support to the notion that *GLUD2* mainly influences aspects of metabolism different from glutamate recycling. We detect no effects on glutamate concentrations in the mouse frontal cortex and our previous results show that glutamate concentrations do not differ between macaques and chimpanzees throughout prefrontal cortex developmental and adult stages, even though chimpanzees carry a *GLUD2* gene. Instead, metabolic differences between $GLUD2^{+}$ and control mice center on the metabolic pathways surrounding the TCA cycle. In agreement with this, it has been reported that overexpression of human *GLUD2*, but not *GLUD1*, in mutant murine glioma progenitor cells results in shunting of carbon into lipid biosynthesis via the TCA cycle (12). Our data further show that metabolic differences between $GLUD2^{+}$ and control mice, as well as between humans and macaques, are particularly prevalent at early developmental stages characterized by rapid brain growth. Given that lipids comprise more than 50% of the brain's dry weight (34), we speculate that *GLUD2* may support the rapid growth of the large ape and human brains by enhancing lipid biosynthesis.

Materials and Methods

A detailed description of materials and methods is provided in *SI Appendix*. Briefly, a human bacterial artificial chromosome containing the *GLUD2* gene (RP11-610G22) was linearized by NotI and injected into the male pronucleus of C57BL/6 mice to construct $GLUD2^{+/-}$ transgenic mice. Transgenic animals were identified by PCRs targeting the 5′-end, the coding region, and the 3′-end of the gene. For metabolome analysis, CE-MS measurements were conducted in frontal cortex samples of 81 control and 56 transgenic mice and prefrontal cortex samples of 35 humans and 34 rhesus macaques. Transcriptome analysis was conducted in the frontal cortex of 29 control and 30 transgenic mice used for metabolite profiling on the Illumina platform, as well as in prefrontal cortex of 38 humans and 40 rhesus macaques (14). Written consent for the use of human tissues for research was obtained from all donors or their next of kin. Use of human autopsy tissue is considered nonhuman subject research and is institutional review board exempt under NIH guidelines. Biomedical Research Ethics Committee of Shanghai Institutes for Biological Sciences completed the review of the use and care of the animals in the research project (approval ID: ER-SIBS-260802P).

ACKNOWLEDGMENTS. We thank Rowina Voigtländer and the staff of the Max Planck Institute for Evolutionary Anthropology's animal facility for expert mouse care; Wulf Hevers and Ines Bliesener for help in preparation of mouse samples; Dr. H. R. Zielke and Dr. J. Dai for providing the human samples; C. Lian, H. Cai, and X. Zheng for providing the macaque samples; J. Boyd-Kirkup for editing the manuscript; Z. He for assistance; and all members of the Comparative Biology Group in Shanghai for helpful discussions and suggestions. This study was supported by the Eunice Kennedy Shriver National Institute of Child Health and Human Development Brain and Tissue Bank for Developmental Disorders; the Netherlands Brain Bank; the Chinese Brain Bank Center; the Suzhou Drug Safety Evaluation and Research Center; the Strategic Priority Research Program of the Chinese Academy of Sciences (Grant XDB13010200 to P.K.); the National Natural Science Foundation of China (Grants 91331203 and 31420103920 to P.K.); the National One Thousand Foreign Experts Plan (Grant WQ20123100078 to P.K.); the National Natural Science Foundation of China (Grant 31401065 to S.G.); the Max Planck Society; and the Paul G. Allen Family Foundation (S.P.).

1. Shashidharan P, et al. (1994) Novel human glutamate dehydrogenase expressed in neural and testicular tissues and encoded by an X-linked intronless gene. *J Biol Chem* 269(24):16971–16976.
2. Fonnum F (1984) Glutamate: A neurotransmitter in mammalian brain. *J Neurochem* 42(1):1–11.
3. Orrego F, Villanueva S (1993) The chemical nature of the main central excitatory transmitter: A critical appraisal based upon release studies and synaptic vesicle localization. *Neuroscience* 56(3):539–555.
4. Burki F, Kaessmann H (2004) Birth and adaptive evolution of a hominoid gene that supports high neurotransmitter flux. *Nat Genet* 36(10):1061–1063.
5. Dupanloup I, Kaessmann H (2006) Evolutionary simulations to detect functional lineage-specific genes. *Bioinformatics* 22(15):1815–1822.
6. Plaitakis A, Spanaki C, Mastorodemos V, Zaganas I (2003) Study of structure-function relationships in human glutamate dehydrogenases reveals novel molecular mechanisms for the regulation of the nerve tissue-specific (GLUD2) isoenzyme. *Neurochem Int* 43(4-5):401–410.
7. Kanavouras K, Mastorodemos V, Borompokas N, Spanaki C, Plaitakis A (2007) Properties and molecular evolution of human GLUD2 (neural and testicular tissue-specific) glutamate dehydrogenase. *J Neurosci Res* 85(5):1101–1109.
8. Rosso L, Marques AC, Reichert AS, Kaessmann H (2008) Mitochondrial targeting adaptation of the hominoid-specific glutamate dehydrogenase driven by positive Darwinian selection. *PLoS Genet* 4(8):e1000150.
9. Kotzamani D, Plaitakis A (2012) Alpha helical structures in the leader sequence of human GLUD2 glutamate dehydrogenase responsible for mitochondrial import. *Neurochem Int* 61(4):463–469.
10. Shashidharan P, Plaitakis A (2014) The discovery of human of GLUD2 glutamate dehydrogenase and its implications for cell function in health and disease. *Neurochem Res* 39(3):460–470.
11. Plaitakis A, Latsoudis H, Spanaki C (2011) The human GLUD2 glutamate dehydrogenase and its regulation in health and disease. *Neurochem Int* 59(4):495–509.
12. Chen R, et al. (2014) Hominoid-specific enzyme GLUD2 promotes growth of IDH1R132H glioma. *Proc Natl Acad Sci USA* 111(39):14217–14222.
13. Bryk J (2009) How to Make an Ape Brain: A Transgenic Mouse Model of Brain Glutamate Metabolism in Humans and Apes. PhD thesis (Max Planck Institute for Evolutionary Anthropology, Leipzig, Germany).
14. He Z, Bammann H, Han D, Xie G, Khaitovich P (2014) Conserved expression of lincRNA during human and macaque prefrontal cortex development and maturation. *RNA* 20(7):1103–1111.
15. Tabas-Madrid D, Nogales-Cadenas R, Pascual-Montano A (2012) GeneCodis3: A non-redundant and modular enrichment analysis tool for functional genomics. *Nucleic Acids Res* 40(Web Server ssue):W478–W483.
16. Shim S, Kwan KY, Li M, Lefebvre V, Sestan N (2012) Cis-regulatory control of corticospinal system development and evolution. *Nature* 486(7401):74–79.
17. Bhattaram P, et al. (2010) Organogenesis relies on SoxC transcription factors for the survival of neural and mesenchymal progenitors. *Nat Commun* 1:9.
18. Mu L, et al. (2012) SoxC transcription factors are required for neuronal differentiation in adult hippocampal neurogenesis. *J Neurosci* 32(9):3067–3080.
19. Wang Y, Lin L, Lai H, Parada LF, Lei L (2013) Transcription factor Sox11 is essential for both embryonic and adult neurogenesis. *Dev Dyn* 242(6):638–653.
20. Jankowski MP, Cornuet PK, McIlwrath S, Koerber HR, Albers KM (2006) SRY-box containing gene 11 (Sox11) transcription factor is required for neuron survival and neurite growth. *Neuroscience* 143(2):501–514.
21. Hide T, et al. (2009) Sox11 prevents tumorigenesis of glioma-initiating cells by inducing neuronal differentiation. *Cancer Res* 69(20):7953–7959.
22. Le TN, et al. (2007) Dlx homeobox genes promote cortical interneuron migration from the basal forebrain by direct repression of the semaphorin receptor neuropilin-2. *J Biol Chem* 282(26):19071–19081.
23. Tanaka S, et al. (2004) Interplay of SOX and POU factors in regulation of the Nestin gene in neural primordial cells. *Mol Cell Biol* 24(20):8834–8846.
24. Kim HD, et al. (2011) Class-C SOX transcription factors control GnRH gene expression via the intronic transcriptional enhancer. *Mol Endocrinol* 25(7):1184–1196.
25. Paina S, et al. (2011) Wnt5a is a transcriptional target of Dlx homeogenes and promotes differentiation of interneuron progenitors in vitro and in vivo. *J Neurosci* 31(7):2675–2687.
26. Iyer AK, Miller NL, Yip K, Tran BH, Mellon PL (2010) Enhancers of GnRH transcription embedded in an upstream gene use homeodomain proteins to specify hypothalamic expression. *Mol Endocrinol* 24(10):1949–1964.
27. Colasante G, et al. (2008) Arx is a direct target of Dlx2 and thereby contributes to the tangential migration of GABAergic interneurons. *J Neurosci* 28(42):10674–10686.
28. de Melo J, et al. (2008) Dlx2 homeobox gene transcriptional regulation of Trkb neurotrophin receptor expression during mouse retinal development. *Nucleic Acids Res* 36(3):872–884.
29. Bergsland M, Werme M, Malewicz M, Perlmann T, Muhr J (2006) The establishment of neuronal properties is controlled by Sox4 and Sox11. *Genes Dev* 20(24):3475–3486.
30. Miller JA, et al. (2014) Transcriptional landscape of the prenatal human brain. *Nature* 508(7495):199–206.
31. Fu X, et al. (2011) Rapid metabolic evolution in human prefrontal cortex. *Proc Natl Acad Sci USA* 108(15):6181–6186.
32. Jewison T, et al. (2014) SMPDB 2.0: Big improvements to the Small Molecule Pathway Database. *Nucleic Acids Res* 42(Database issue):D478–D484.
33. Enard W (2014) Mouse models of human evolution. *Curr Opin Genet Dev* 29:75–80.
34. Piomelli D, Astarita G, Rapaka R (2007) A neuroscientist's guide to lipidomics. *Nat Rev Neurosci* 8(10):743–754.